LATIN AMERICAN CUBESAT WORKSHOP
SALVADOR, BR
OCTOBER 2024

Analysis of the collimation of an electron beam in a Magnetic Mirror for Possible Plasma Thruster Applications

Luis Ángel Fernández Ramos[1] and José Eduardo Mendoza Torres[2]

[1]Space Science and Technology Postgraduate Program, Instituto Nacional de Astrofísica, Óptica y Electrónica
[2]Department of Astrophysics, Instituto Nacional de Astrofísica, Óptica y Electrónica

Abstract

In this paper, we study the dynamics of an electron beam inside a magnetic bottle when a constant electric field parallel to the bottle axis is applied, we use Particle-in-Cell (PIC) simulations with a 1D-3V model in z direction. It is considered that the electron beam has a temperature of 1 eV and follows a Maxwellian distribution function. We study two different cases. In the first case, the electron beam is injected inside an annular device which consists of two stages. In the first stage, called the acceleration stage, the electrons are accelerated by a constant electric field parallel to the bottle axis for a distance equal to half the total length of the annular channel of the device. Then, the accelerated electrons enter a magnetic bottle in order to control the beam divergence and reduce its mobility perpendicular to the magnetic field. This stage is called the collimation stage. In this stage, we consider the force exerted by the magnetic field gradient on the electrons. For the second case, we study the response of the electrons when the electric field and the magnetic bottle span the entire length of the annular channel. In both cases, the electric and magnetic fields point in z direction. For simplicity, we do not consider the electric fields that could be generated by charge separation or density gradients. Finally, we also study the behavior of those electrons that fulfilled the reflection condition and are trapped between both fields.

Keywords: Electric Thruster, Magnetic Bottle, Particle in Cell, Plasma

1 Introduction

Electric thrusters are used for small satellites, as Cubesat, and also for deep space missions. In the case of small satellites, this type of thruster is used for orbit correction, since the atmosphere interaction with the satellites produces changes in their orbit. One of the types of thrusters suitable for this purpose is the Hall effect thruster, which is very efficient. Although its thrust is small, it is also used for missions requiring long distances. In Hall thrusters, keeping the electrons in a given area is important to ionize the atoms that serve as fuel. The magnetic system of the thruster generates a magnetic field, similar to a magnetic bottle, which allows the confinement of the electrons. However, some instabilities cause a number of the electron population to leave this confinement, which decreases both the thruster's thrust and its lifetime.

Let us consider a magnetic field that points mainly in *z* direction and its magnitude varies in the same direction. Let us consider, also, that the field is axisymmetric with $B_\theta = 0$ and without azimuthal variations $\partial/\partial\theta = 0$. The magnetic field must have a radial component B_r that allows the convergence of the field lines. This magnetic field topology is commonly known as a magnetic bottle.

The force that a charged particle experiences in this field is due to the Lorentz force that, in cylindrical coordinates, is represented as

$$F_z = e\left(v_\theta B_r - v_r B_\theta\right) \quad (1)$$
$$F_r = e\left(v_z B_\theta - v_\theta B_z\right) \quad (2)$$
$$F_\theta = e\left(v_r B_z - v_z B_r\right) \quad (3)$$

Since the components F_r and F_θ only produce the cyclotron motion, we are interested in analyzing the electron motion due to the axial component of the magnetic force F_z. Due to the symmetry, the component $B_\theta =$, and only the radial component of the magnetic field B_r needs to be found through divergence of the magnetic field, which in cylindrical coordinates is represented as

$$\vec{\nabla} \cdot \vec{B} = \frac{1}{r}\frac{\partial(rB_r)}{\partial r} + \frac{1}{r}\frac{\partial B}{\partial \theta} + \frac{\partial B}{\partial z} \quad (4)$$

It can be shown that if $\partial B_z/\partial z$ does not vary much with r, the radial component of the magnetic field can be expressed as

$$B_r = -\frac{1}{2}r\frac{\partial B}{\partial z} \quad (5)$$

Once the magnetic field components are known, we can use the momentum equation to analyze the movement of the electrons

$$\frac{d\vec{v}}{dt} = \frac{e}{m_e}\left(\vec{E} + \vec{v} \times \vec{B}\right) - \frac{1}{m_e n_e}\vec{\nabla} P_e$$

$$-\nu_{en}\left(\vec{v}_e - \vec{v}_n\right) \quad (6)$$

where $\vec{v}_e$ is the velocity vector of the electrons, $\vec{E}$ is the electric field, P_e is the pressure term, $\vec{B}$ is the magnetic field vector, e and m_e are the charge and mass of the electron, n_e is the electron number density, ν_{en} is the collision frequency between electrons and neutral atoms and $\vec{v}_n$ is the neutral bulk velocity.

We consider a collisionless, cold plasma, therefore, the momentum equation in (6) takes the form

$$\frac{d\vec{v}}{dt} = \frac{e}{m_e}\left(\vec{E} + \vec{v} \times \vec{B}\right) \quad (7)$$

Equation (7) can be expanded into a set of differential equations of the form

$$\frac{dv_z}{dt} = \frac{e}{m_e}\left(E_Z + (v_\theta B_r - v_r B_\theta)\right) \quad (8)$$

$$\frac{dv_r}{dt} = \frac{e}{m_e}\left(E_r + (v_z B_\theta - v_\theta B_z)\right) \quad (9)$$

$$\frac{dv_\theta}{dt} = \frac{e}{m_e}\left(E_\theta + (v_r B_z - v_z B_r)\right) \quad (10)$$

Since we are interested in the motion of the electrons parallel to the axis of the magnetic bottle, we only need to solve the axial component of motion (8). Due to the assumption of the axisymmetric field concerning the azimuthal coordinate, then, only the radial coordinate of the magnetic field needs to be substituted, such that

$$\frac{dv_z}{dt} = \frac{e}{m_e}E_z - \frac{1}{2}\frac{e}{m_e}v_\theta r\left(\frac{\partial B}{\partial z}\right) \quad (11)$$

where the dependence on B_θ was removed due to the axisymmetric geometry. If we consider that $v_\theta \approx c$ during the gyromotion, $v_\theta = v_\perp$.Furthermore, since r represents the Larmor radius, then the axial component of the momentum equation can be represented as

$$\frac{dv_z}{dt} = \frac{e}{m_e}E_z - \frac{1}{m_e}\mu\left(\frac{\partial B}{\partial z}\right) \quad (12)$$

In (12) we have used the mathematical definition of the Larmor radius $r_L = v_\perp/\omega_{ce}$, where $\omega_{ce} = eB/m_e$ is the cyclotron frequency, and we have also substituted the equation for the magnetic moment $\mu = m_e v_\perp^2/2B$. The expression found for the momentum equation in (12) allows us to know the motion of the electrons parallel to the axis of the bottle, furthermore, the force produced by the field gradient is opposite to the motion of the particle, similar to the force acting on a diamagnetic particle.

The magnetic field described above is used as one of the main schemes for plasma confinement. Confinement is possible due to the invariance of the magnetic moment, however, not all electrons entering the bottle are confined. The confinement depends on the ratio of the maximum value B_m to the minimum value B_0 of the magnetic field called the mirror ratio $R = B_m/B_0$, and the angle formed by the velocity vector with respect to the magnetic field called the pitch angle. A more detailed explanation of plasma confinement and magnetic moment invariance can be found in [1] and [2]. A consequence of the magnetic bottle structure is the decrease in the area initially covered by the electron beam as it moves to regions of higher intensity. The relationship between the initial area covered by the beam and the final area can be obtained using the definition of magnetic moment and its relationship to the magnetic field. The magnetic moment generated by an electric current is given by

$$\mu = IA \quad (13)$$

where I is the current generated due to the trajectory of the charged particle around the magnetic field line and A is the area formed by the cyclotron motion. This area is characterized by the Larmor radius. If we use (13) and the magnetic moment definition (12), we obtain

$$IA = \frac{1}{2}\frac{m_e v_\perp^2}{B} \quad (14)$$

It can be shown that the following equation is fulfilled.

$$\frac{B_0}{B_m} = \frac{A_m}{A_0} \quad (15)$$

where B_0 and B_m are the minimum and maximum values of the magnetic field, while A_0

and A_m represent the area covered by the electron beam in the regions of minimum and maximum magnetic field. For a more detailed explanation see [3].

2 Problem Description

We simulated two different cases in order to analyze the dynamics of an electron beam in a magnetic bottle. In both cases, the electron beam enters an annular channel device through which a constant electric field is applied, parallel to the axis of the bottle, both in the z direction. According to the assumptions of the theory described in the previous section, the only forces acting on the electrons will be the electric force and the force generated by the axial gradient of the magnetic field.

In the first case, two different stages are considered during the trajectory of the electrons. In the first stage, called the acceleration stage, the electron beam is accelerated for half the length of the channel due to a constant electric field in the axial direction. Then, the electrons enter inside a magnetic bottle, in the axial direction, to reduce the divergence of the beam. This stage is called the collimation stage. In this case, the electric and magnetic field gradient forces are considered separately.

In the second case, the electric and magnetic fields are applied along the entire channel, and the beam dynamics are analyzed when both forces act at the same time, following the mathematical model described in the previous section.

To study both cases, we used 1D-3V Particle in Cell simulations, in the axial direction. In the first part of the code, we designed the simulation domain. The domain length L, which represents the channel length, was $L = 0.115$ m with a spatial resolution Δx, and temporal resolution Δt, which follow the criteria established in [4]. We can compute $\Delta x < \lambda_D$ where λ_D is the Debye Length and $\Delta t < 0.2/\omega_{pe}$ where ω_{pe} is the electron plasma frequency. We used a one-dimensional exponential model to generate the bottle, however, because the one-dimensional model cannot capture the convergence of magnetic field lines, the gradient force must be explicitly added to simulate the confinement. The model used for the magnetic field was [5].

$$B = \exp\left(-2(z-1)^2\right) + \exp\left(-2(z+1)^2\right) \tag{16}$$

with $z = z_0/L$ with z in [-1,1] where z_0 is the electron position and L the domain length. The mathematical model for the magnetic field gradient was obtained by deriving the above equation

$$\frac{\partial B}{\partial z} = \left[-4(z-1)(\exp\left(-2(z-1)^2\right)\right] - \left[-4(z+1)(\exp\left(-2(z-+)^2\right)\right] \tag{17}$$

From (16) it is easy to see that the magnetic field has its maximum for z=1 and the minimum for $z = 0$, which gives a mirror ratio $R \approx 3.70$. This mirror ratio reduces the initial area covered by the electrons, in the same proportion. The next step was to create the electron beam, assuming that the electrons follow a Maxwellian distribution and are uniformly distributed throughout the simulation domain. The number of macroparticles per cell of the domain must follow the criterion $N_{cell} > 50$ [4]. The criterion of the number of macroparticles per cell is not as severe as the temporal and spatial restrictions, especially when high plasma densities are involved because the charge separation and motions on the order of the plasma frequency or even the cyclotron frequency must be solved. To get a better idea of the stringency of the restrictions, suppose a plasma of density $n \approx 1 \times 10^{18} m^{-3}$ with an electron temperature of $T \approx 20$ eV (approximate conditions of a Hall thruster), the spatial resolution, for these conditions, requires that $\Delta x < 20 \mu m$, while the temporal resolution, to solve the cyclotron motion, requires that $\Delta t < 2 \times 10^{-12}$ sec, for this reason, one must be careful when selecting the characteristics of the plasma to be studied.

3 PIC Simulations

We use a fully kinetic simulation which resolves the motion of electrons around magnetic field lines. Although we are interested in the motion of particles in the direction of the magnetic field, we need to solve the perpendicular component of the velocity at each integration step to maintain the invariance of the magnetic moment. We use the Boris method to integrate the velocity in the presence of the magnetic field, such that

$$\frac{\vec{v}^{k+0.5} - \vec{v}^{k-0.5}}{\Delta t} = \frac{q}{m} \vec{E}^k + \frac{\vec{v}^{k+0.5} - \vec{v}^{k-0.5}}{2} \times \vec{B}^k \quad (18)$$

where k represents the current time, q and m the charge and mass of the particle, respectively, and Δt is the time resolution. Boris's method effectively solves the magnetization of electrons and conserves energy by eliminating the electric field by defining a new pair of variables

$$\vec{v}^{k-0.5} = \vec{v}^{-} - \frac{q}{m} \vec{E}^k \frac{\Delta t}{2} \quad (19)$$

$$\vec{v}^{k+0.5} = \vec{v}^{+} + \frac{q}{m} \vec{E}^k \frac{\Delta t}{2} \quad (20)$$

with these substitutions a pure rotations is obtained

$$\frac{\vec{v}^{+} - \vec{v}^{-}}{\Delta t} = \frac{q}{2m} \left(\vec{v}^{+} + \vec{v}^{-} \times \vec{B}^k \right) \quad (21)$$

where the angle of rotation is

$$\tan\left(\frac{\theta}{2}\right) = -\frac{q}{m} \frac{\Delta t}{2} B \quad (22)$$

and the rotation vector can be written as

$$\vec{t} = -\hat{b} \tan\left(\frac{\theta}{2}\right) \quad (23)$$

We can use (22) to obtain the first rotation of the velocity vector

$$\vec{v}' = \vec{v}^{-} + \vec{v}^{+} \times \vec{t} \quad (24)$$

Equation (23) rotates the velocity vector $\Delta t/2$. For the next rotation, we scale the magnitude to maintain the magnitude of the velocity

$$\vec{v}^{+} = \vec{v}^{-} + \vec{v}' \times \vec{s} \quad (25)$$

where the vector $\vec{s}$ is

$$\vec{s} = \frac{s\vec{t}}{1 + t^2} \quad (26)$$

Since we are simulating a one-dimensional model, the gradient force must be added explicitly to the Boris method, in order to capture the reflection of the electrons, such that the variables $\vec{v}^{+}$ and $\vec{v}^{-}$ are obtained using the following expressions

$$\vec{v}^{-} = \vec{v}^{k+0.5} + \frac{\Delta t}{2m} \left(q\vec{E}^k - \mu^k \frac{\partial B}{\partial z} \right) \quad (27)$$

and

$$\vec{v}^{k+0.5} = \vec{v}^{+} + \frac{\Delta t}{2m}\left(q\vec{E}^{k} - \mu^{k}\frac{\partial B}{\partial z}\right) \tag{28}$$

Once the new velocities are known, the new positions are obtained

$$\vec{x}^{k+1} = \vec{x}^{k} + \vec{v}^{k+0.5}\Delta t \tag{29}$$

In this case we only update the axial position. The method described above can be summarized with the next sequence of steps:

1. Compute the magnetic field B in the particle position in the time k using (16).
2. Compute the magnetic moment μ of the particle i in the time k.
3. Compute the magnetic gradient $\partial B/\partial z$ in the particle position in the time k using (17).
4. Compute $\vec{v}^{-}$ using $\vec{v}^{k-0.5}$ using (25).
5. Compute the first half rotation $\vec{v}'$ using (23).
6. Compute the second half rotation $\vec{v}^{+}$ using (24).
7. Compute $\vec{v}^{k+0.5}$ using (26).
8. Update the particle position using Leap-Frog (27).

4 Results

The simulations were done at the LABORATORIO NACIONAL DE SUPERCÓMPUTO DEL SURESTE DE MÉXICO (LNS) of the Benemérita Universidad Autónoma de Puebla (BUAP). For both cases, an electron beam with a numerical density $n = 1 \times 10^{12} m^{-3)}$ and a temperature $T = 1$ eV was simulated. A maximum magnetic field of $B_{max} = 300$ Gauss and an electric potential $\phi = 300$ V were used. For these characteristics, the stability criteria, i.e., the conditions for not having values generated by computational errors in the simulation process, require that $\Delta x < 7 \times 10^{-3}$ m and $\Delta t < 2{\times}10^{-10}$ sec. The values used for spatial and temporal resolution were $\Delta x = 2 \times 10^{-3}$ m and $\Delta t = 1 \times 10^{-10}$ sec. The spatial resolution leaves a total of 58 nodes and 57 cells, so 2875 macroparticles were simulated. In both cases, the electron beam was uniformly distributed along the domain.

For the first case, we simulated a total time of $t = 15\mu s$ corresponding to 75000-time steps (vertical axis of the left panels of Fig. 1). We analyzed the behavior of the electron beam through the numerical density and the evolution of the velocity distribution function. We developed four simulations associated with Fig. 1 to Fig. 4, the reason why the velocity distribution of the electrons is slightly different in each figure, is a consequence of the generation of random numbers, however, the initial conditions for each simulation were the same. The simulations show the formation of two populations of electrons along the domain (Fig. 2), with approximately the same number of particles. The fast population represents those electrons accelerated by the electric field, and the slow population is associated with those electrons placed inside the bottle without being accelerated before.

Another important phenomenon is the accumulation of electrons that forms right in the middle of the channel from iteration 7500, once both populations are fully visualized. This accumulation travels along the domain, and near iteration 40000, the population of fast

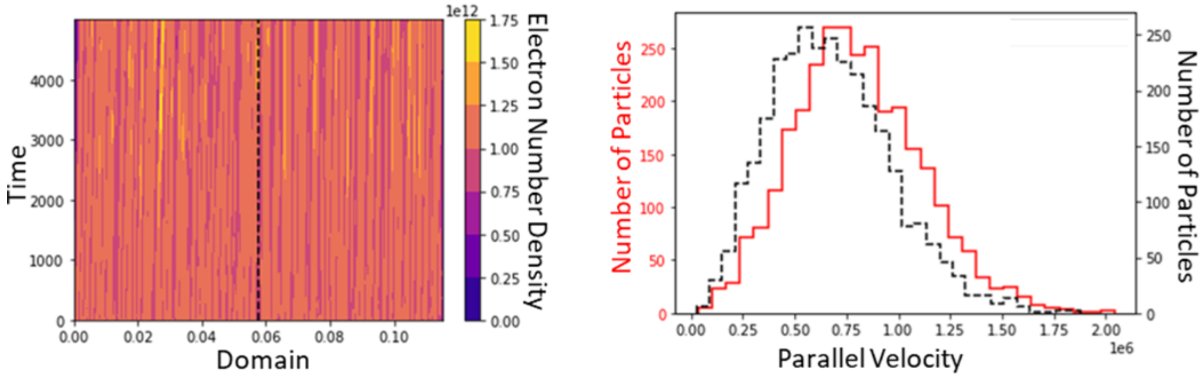

Figure 1: **Left.** Representation of the electron density for different times as a function of the position in the spatial domain. On the y-axis, the time expressed in terms of iterations is represented. On the x-axis, the spatial domain is represented by a position within the channel. The colors represent the density according to the bar on the right side. This particular case corresponds to the time $t = 5000$ iterations. The dashed line corresponds to the location where the fields separate. **Right.** Velocity distributions for the initial time of the simulation (black line) and, for the final time (red line). The scales corresponding to each distribution are shown with the corresponding colors. On the x-axis, the velocity of the electrons is represented in a direction parallel to the axis of the magnetic bottle. It can be seen that the velocity values cover a range from 0 to 2×10^6 m/s

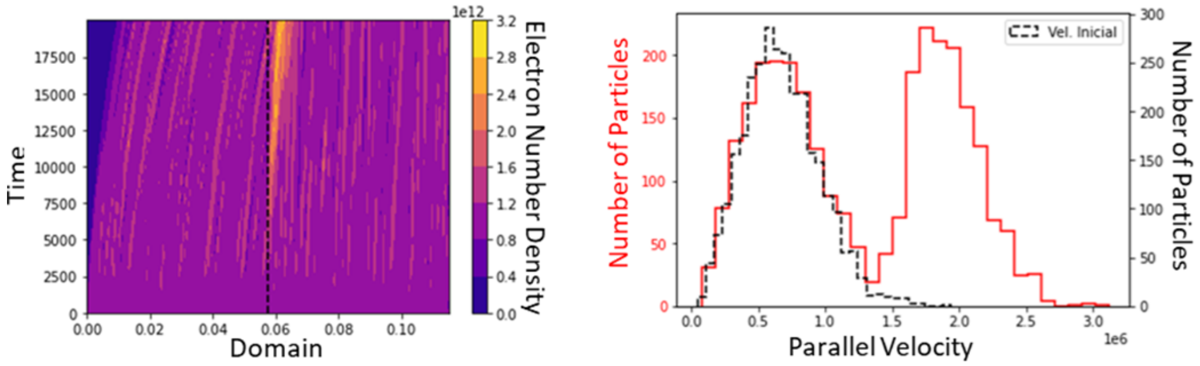

Figure 2: **Left.** Like Figure 1, the left panel shows the number density of electrons. This particular case corresponds to the time $t = 20000$ iterations. The dashed line corresponds to the location where the fields separate. **Right.** For this specific case, a third velocity distribution (red line) can be observed. This distribution is associated with a population of fast electrons, which was accelerated by the electric field.

electrons decreases due to the exit of electrons from the channel and the force due to the gradient, which slows down their movement. In fact, in the left panel of Fig. 3 between

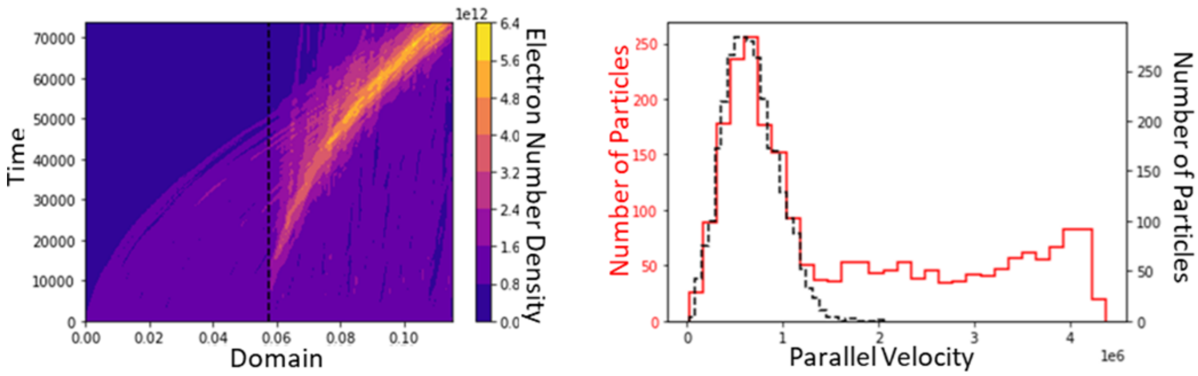

Figure 3: **Left.** Like Figure 1, the left panel shows the number density of electrons. This particular case corresponds to the time $t = 75000$ iterations. The dashed line corresponds to the location where the fields separate. **Right.** A decrease in the fast electron population is observed. This decrease is associated with the fact that some fast electrons have escaped from confinement.

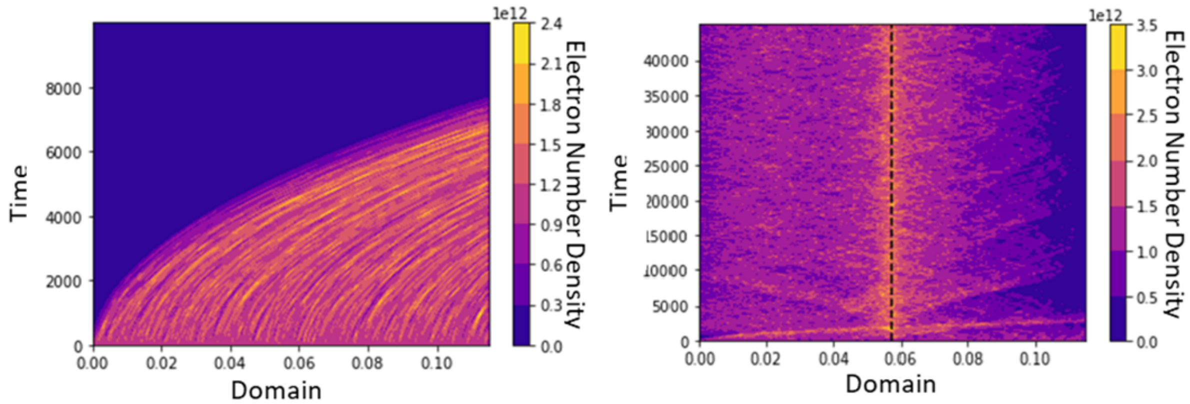

Figure 4: **Left.** Representation of the electron density for different times as a function of the position in the spatial domain. On the y-axis, the time expressed in terms of iterations is represented. On the x-axis, the spatial domain is represented by a position within the channel. The colors represent the density according to the bar on the right side. This particular case corresponds to the time $t = 10000$ iterations. **Right.** Representation of the electron density for different times as a function of the position in the spatial domain. On the y-axis, the time expressed in terms of iterations is represented. On the x-axis, the spatial domain is represented by a position within the channel. The colors represent the density according to the bar on the right side. This particular case corresponds to the time $t = 45000$ iterations. The dashed line corresponds to the location where an accumulation of electrons is observed.

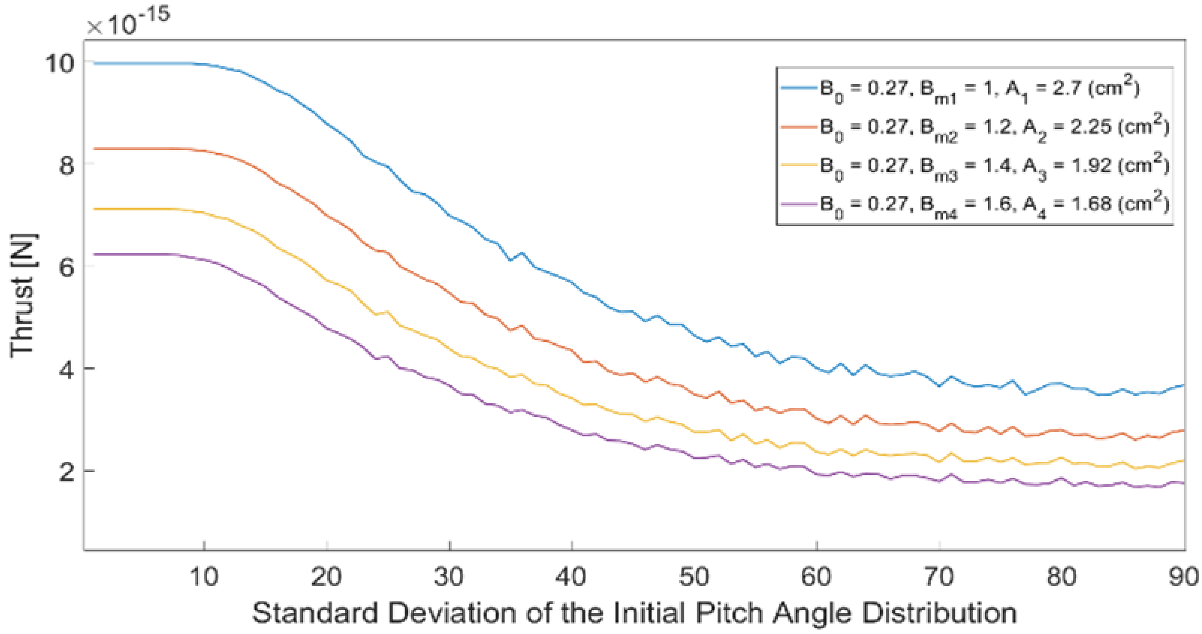

Figure 5: Values corresponding to Case 2. Thrust generated by the electron beam after being accelerated, for different values of the mirror ratio. In the x-axis, the dispersion of the pitch angle is represented by a standard deviation of the initial distribution for 2875 electrons. The parameter A corresponds to the area the electrons cover after being collimated.

the values 0.6 and 0.8 of the horizontal axis, between iteration 20000 – 50000, almost vertical lines can be seen associated with those electrons that experienced accelerations in a small-time interval, that is, they were very close to the entrance to the magnetic bottle, such that when entering this region, the force due to the magnetic field gradient could produce their deceleration, confining them inside the bottle. Furthermore, the histogram in Fig. 3 shows a dramatic reduction in the population of fast electrons, suggesting that electrons with higher velocities escape from confinement. These points are supported by the fact that, out of 2875 simulated electrons, 1321 escaped, a value that represents less than 50%.

For the second case, we performed two simulations. In the first simulation, we used the same values as the first case for the magnetic field and the electric potential. The simulation shows that the gradient force is not strong enough to confine the electrons and before 8000 iterations, the electron beam had completely escaped. For the second simulation, we increased the value of the magnetic field, the gradient, and the mirror ratio and found that the electron beam remains confined and bounces between the ends of the bottle. In the right panel of Fig. 4, it can be seen that around iteration 3000, those electrons whose pitch angle was smaller than the critical angle escaped, while all the others were reflected. Areas of lower density can also be seen near the exit of the bottle; this indicates that the reflection of the electrons does not occur precisely in the area of the highest magnetic field intensity.

Finally, we calculate the thrust that can be produced with this number of macroparticles. In practice, it is simpler to calculate thrust using the particle beam current due to the mass flow rate

$$T = \dot{m}v_{ex} = MQv_{ex} = \frac{I_b M v_{ex}}{e} \qquad (30)$$

where T is the thrust, $\dot{m}$ is the mass flow rate, v_{ex} is the exhaust velocity, M is atomic mass, Q is the flow rate and I_b is the beam current.

In Fig. 5 we plot different values of the thrust generated by the electron beam as a function of the pitch angle dispersion, represented as the standard deviation of the angle distribution function, and the inverse mirror ratio. A decrease in thrust can be observed as the mirror ratio increases, this is due to electron confinement. Likewise, if we increase the pitch angle dispersion, the number of confined electrons also increases. A more detailed analysis of this thrust generation process can be found in [3].

5 Discussion

In the previous analysis, we neglected thermal motions and collisions because the velocity of the particles is modified. In addition, those magnetized particles modify their pitch angle also, which causes them to disperse and escape from confinement easily. For the study, it would seem that adding collisions between particles could be beneficial because it would decrease the number of trapped particles, producing more thrust. However, we must remember that the diffusion of the plasma, perpendicular to the magnetic field, is directly proportional to the collision frequency, which could represent a problem of plasma loss due to diffusion. For this reason, the research should be extended to two dimensions and the use of other mathematical models to simulate the magnetic bottle, or failing that, other collimation methods, in order to quantify the loss of thrust as a consequence of electron trapping or diffusion processes, as well as the effects of the model on the accumulation of particles in some regions, to find physically more precise results. This last point is important because this accumulation can generate instabilities in the plasma and thrust reduction.

Conclusions

Applying the electric and magnetic fields separately generates the formation of a third population of electrons that escape from the bottle. This new population produces the thrust. To prevent a certain part of the electrons from being confined and losing thrust, the electrons must be accelerated from the left boundary of the domain (which represents the entrance to the thruster channel), otherwise, a large part of the simulated particles (approximately 50%) will be trapped in the bottle. The shift of the maximum value of the number density in Fig. 1 to Fig. 3 allows us to get an idea of the number of particles trapped in the bottle. The application of the magnetic bottle allows us to obtain a reduction of the area initially covered by the electrons, according to (15).

From the left panel of Fig. 4, we can conclude that all the electrons escape from the bottle to produce thrust but, if the magnetic field intensity is increased (right panel of Fig. 4), the electron dynamics become more complex because the beam bounces off the domain boundaries, forming regions of high and low electron density. Furthermore, on the right side of the dashed line, in the time interval 5000 - 10000, a slope is formed and increases its steepness in the interval of 5000 iterations. Around iteration 25000, the slope appears to remain constant. This behavior is not perceived on the left side of the dashed line.

A rather interesting pattern is the evolution of the maximum density, tracing a vertical line in yellow corresponding to the highest values in Fig. 4. This region, of high density values, is formed in regions close to the middle of the domain. This phenomenon needs to be studied further to understand the causes and conclude whether it is related to the mathematical model.

Acknowledgment

Luis Ángel Fernández Ramos wants to thank Consejo Nacional de Humanidades, Ciencia y Tecnología (CONAHCYT) for the postgraduate grant. The authors thank Benemérita Universidad Autónoma de Puebla (BUAP) for allowing the use of Laboratorio Nacional de Supercómputo del Sureste de México (LNS) for the time allocated to do a series of simulations that served to obtain some of the results presented in this work.

References

[1] F. F. Chen, *Introduction to Plasma Physics and Controlled Fusion*. Springer, 2016.

[2] L. Ángel Fernández J. E. Mendoza Torres O. Gomez Flores and E. T. Bueno, "Charged particle reflection in a magnetic mirror," *Rev. Mex. Fis. E*, 2024.

[3] L. Ángel Fernández J. E. Mendoza Torres, "Thrust generation through a collimated electron beam in a magnetic mirror and its possible applications in plasma thrusters," *International Journal of Engineering and Advanced Technology*, 2024.

[4] J. P. Boeuf, "Tutorial: Physics and modeling of hall thrusters," *J. Appl. Phys.*, 2017.

[5] L. Brieda, *Plasma Simulations by Example*. CRC Press, 2019.